*Marius Dotter[1], Lion Lukas Placke[1], Jan Lukas Storck[1], Uwe Güth[2]*
*[1] Faculty of Engineering and Mathematics, Bielefeld University of Applied Sciences, 33619 Bielefeld, Germany*
*[2] Department of Physical and Biophysical Chemistry (PC III), Faculty of Chemistry, Bielefeld University, 33615 Bielefeld, Germany*

# Characterization of PAN-$TiO_2$ Nanofiber Mats and their Application as Front Electrodes for Dye-sensitized Solar Cells

## *Karakterizacija PAN-$TiO_2$ nanovlaknatih kopren in njihova uporaba kot sprednjih elektrod za elektrokemijske sončne celice*

Original scientific article/*Izvirni znanstveni članek*
Received/*Prispelo* 10-2022 • Accepted/*Sprejeto* 12-2022

Corresponding author/*Korespondenčni avtor:*
**Marius Dotter, MSc**
E-mail: marius.dotter@fh-bielefeld.de
Tel.: +4952110670934
ORCID ID: 0000-0001-8398-1809

## Abstract

In the context of the energy transition to renewables, the spotlight is on large systems connected to the power grid, but this also offers room for smaller, more specialized applications. Photovoltaics, in particular, offer the possibility of the self-sufficient supply of smaller electrical appliances on smaller scales. The idea of making previously unused surfaces usable is by no means new, and textiles such as backpacks, tent tarpaulins and other covers are particularly suitable for this purpose. In order to create a non-toxic and easily recyclable product, dye-sensitized solar cells (DSSC), which can be manufactured through electrospinning with a textile feel, are an attractive option here. Therefore, this paper investigates a needle electrospun nanofiber mat, whose spin solution contains polyacrylonitrile (PAN) dissolved in dimethyl sulfoxide (DMSO) as well es $TiO_2$ nanoparticles. In addition to characterization, the nanofiber mat was dyed in a solution containing anthocyanins to later serve as a front electrode for a dye-sensitized solar cell. Although of lower efficiency, the DSSC provides stable results over two months of measurement.
Keywords: dye-sensitized solar cells (DSSC), long-term stability, electrospinning, polyacrylonitrile (PAN), $TiO_2$ nanoparticles

## *Izvleček*

*V okviru energetskega prehoda na obnovljive vire so v središču pozornosti veliki sistemi, povezani z električnim omrežjem, vendar pa je tu tudi prostor tudi za manjše, specializirane aplikacije. Predvsem fotovoltaika ponuja možnosti za samozadostno oskrbo manjših električnih naprav z manjšim obsegom. Zamisel o uporabi prej neizkoriščenih površin ni nova, za ta namen pa so še zlasti primerni izdelki iz tekstilij, kot so nahrbtniki, ponjave za šotore in druga pregrinjala. Za razvoj nestrupenega izdelka, ki ga je mogoče zlahka reciklirati, so tukaj privlačna možnost elektrokemijske sončne celice, ki jih je mogoče izdelati z elektropredenjem in ki imajo tekstilni otip. Zato je v tem članku raziskana nanovlaknata koprena, izdelana v enoigelnem postopku elektropredenja iz raztopine poliakrilonitrila (PAN), raztopljenega v dimetilsulfoksidu (DMSO), z dodatkom nanodelcev $TiO_2$. Poleg karakterizacije je bila nanovlaknata koprena tudi barvana v raztopini antocianov, da bi bila pozneje uporabljena kot sprednja elektroda za elektrokemijsko sončno celico. Čeprav je manj učinkovita, pa je elektrokemijska elektroda pri dvomesečnem merjenju zagotovila stabilne rezultate.*
*Ključne besede: elektrokemijske sončne celice, dolgotrajna stabilnost, elektropredenje, poliakrilonitril (PAN), nanodelci $TiO_2$*

## 1 Introduction

Although the negative effects of conventional, primary methods of energy production such as coal and nuclear energy are well known, the development and expansion of renewable energy sources are not progressing fast enough [1]. New energy sources are not only suitable for replacing currently used sources by large-scale installations with power grid feed-in, but also offer further, special application areas for buildings or private use [2], for example existing tablet-sized photovoltaic systems for mobile use. Of course, the latter application will not cover broader energy demand, but small, decentralized devices for energy harvesting provide energy where otherwise previously charged accumulators or batteries would be used or it is otherwise difficult to install larger systems. This concept will be addressed here with an attempt to make textiles usable for energy production in everyday life. Here, tent/pavilion tarpaulins, backpacks and sunshades can serve as carriers for a dye-sensitized solar cell (DSSC) with textile haptics [3].

In a DSSC, a dye with a suitable orbital structure serves as a light absorber. The dye is classically bonded to a semiconductor, which slightly shifts the energetic structure and thus the colour of the dye. The dye releases electrons through light absorption, whereby the dye becomes positive and no longer active until its regeneration. Similar to normal silicon cells, this absorber layer is located on a light-transmissive, conductive layer in order to transport the current away. Usually, indium tin oxide (ITO) on glass is used for the latter. Through an external circuit, the electrons reach the back side of the DSSC. There is a catalyst layer, usually graphite or platinum, and an electrolyte matched to the dye. Through a Redox reaction, the dye is regenerated again and is once more available for energy absorption [4, 5].

As a further difference and advantage over conventional silicon-based cells, these DSSCs should be simple and inexpensive to manufacture and non-toxic in order to simplify their recycling [6]. At the same time, refined textiles should provide stability and contacting. A gel electrolyte with long-term stability ensures the good regeneration of the dye and hardly evaporates, which avoids the sealing and possible negation of the textile properties of the cell [3, 7-10]. However, the main focus here is on the simple production of the front electrode. As an alternative to conventional layers, we want to use nanofiber mats for this purpose, since they have the desired textile feel, are stable and flexible, can be customized with the appropriate materials and have a large surface area [11]. Several approaches already exist for producing a functioning front electrode for a DSSC from a nanofiber mat. Kohn et al. describe a multilayer needleless electrospinning process based on polyacrylonitrile (PAN), starting with a catalyst graphite layer, then a buffer layer on top, and finally a nanofiber mat with titanium dioxide ($TiO_2$) and dye already in the spin solution. The multilayer mat is subsequently impregnated with a conductive polymer, dried and then used as a DSSC [3]. However, for simplicity in the development process, usually only one component of the cell is spun, as in Mamun et al. [12]. They first spun a PAN nanofiber mat with $TiO_2$ content using needleless electrospinning, carbonized it for conductivity and then dip-coated it in dissolved anthocyanins. It should be noted that carbonization requires similar temperatures as sintering, and therefore entails similar problems, such as damage to the other layers.

Therefore, the electrospinning of the front electrode was further investigated and its long-term performance measured. In this work, PAN dissolved in dimethyl sulfoxide (DMSO) with suspended $TiO_2$ nanoparticles was spun using a needle electrospinning system, in contrast to previous studies. For this purpose, a previously mixed solution of polymer, solvent and additive was filled into a syringe pump and forced through a small nozzle under a fixed pressure. A high voltage was applied between the nozzle and a collector plate, usually made of aluminium, which draws thin polymer filaments to the collector. A characteristic Taylor cone was formed at the nozzle and the nanofibers were deposited in random orientation on the collector. By using a moving nozzle holder and a rotating collector, the fibres can be given the preferred orientation. The nanofiber mat produced as such was measured using optical and scanning electron microscopy (SEM). In addition, a piece of the nanofiber mat was analysed through thermogravimetric analysis (TGA) to reach conclusions about the PAN to $TiO_2$ ratio. The nanofiber mat was further dip-coated in a solution of dissolved anthocyanins to dye the $TiO_2$ particles via covalent binding and then assembled as a component for a DSSC. In addition, a commercially available liquid electrolyte was used in order to investigate the rapid evaporation of the electro-

lyte in the usual comparison cells. The prepared DSSCs were subsequently measured over a period of about two months.

It should be noted that neither the carbonization of the nanofiber mat nor sintering of the $TiO_2$ was carried out. Since the front electrode is to be spun directly onto existing components of the DSSC in the workflow of future application, thermal treatment, which is necessary for both carbonization and sintering, would negatively affect or even destroy other components of the DSSC.

## 2 Materials and Methods

A suspension containing DMSO (min. 99.9%, obtained from S3 chemicals, Bad Oeynhausen, Germany) as solvent, X-PAN as co-polymer (93.5% acrylonitrile, 6% methylacrylate, 0.5% natrium-sodium-mythallylsulfonate, Dralon, Dormagen, Germany; Mn = 90,000 g/ml, Mw = 250,000 g/mol) and $TiO_2$ nanoparticles with an average size of 21 nm (P25 Titanium IV oxide nanopowder, 21 nm primary particle size, Sigma Aldrich, Saint Louis, MO, USA) in a weight ratio of 8:1:1 was prepared. For this purpose, the X-PAN was dissolved in DMSO for one hour at room temperature while stirring, $TiO_2$ was then added and mixed in. A homogeneous nanofiber mat was electrospun using a SpinBox (Bioinicia, Spain) needle-based electrospinning machine with a horizontally moving nozzle holder and a rotating collector. The spin parameters were as follows: voltage: 25 kV; pump speed: 1000 µl/h; distance nozzle to collector: 20 cm; collector rotation speed: 400 rpm; temperature 21.5 °C; relative humidity: 26%; outer nozzle diameter: 1.6 mm; and duration: 72 min. In addition, a spinning solution of 16 wt% X-PAN dissolved in DMSO was prepared and spun using the same parameters to produce a $TiO_2$-free reference nanofiber mat.

To extract the anthocyanins, 17 g of Maqui berry tea (Mayfair, Wilken Tee GmbH, Fulda, Germany) was mixed with 150 g of deionized water and 50 g of ethanol, stirred for half an hour and subsequently filtered. The now filtered anthocyanin dye solution was placed in a beaker that facilitated the sufficient dip-coating of the nanofiber mats. For immersion during dip-coating, the nanofiber mat was held with metal tongs. This also prevented the nanofiber mat from rolling up due to surface tension. To dye the nanofiber mat, it was then immersed in the dye solution for about 30 s with gentle stirring and afterwards placed on a commercial fluorine-doped tin oxide coated glass slide (ManSolar, Petten, Netherlands) and stored in the dark for drying. In the case of the $TiO_2$ nanofiber mat, this then facilitated direct use as a front electrode for a DSSC after drying.

The structure of the anthocyanin dye is shown in Figure 1. Since there are always many different anthocyanins present as colour, only the general mesomers have been shown. Sugars or similar large structures can be attached as residues, but mostly these are hydroxy or hydrogen groups.

Similar glass slides were used for the counter electrode. The slides were sprayed with a graphite spray (CP-Graphitprodukte GmbH, Wachtberg, Germany) for 1 s from a distance of 50 cm. In addition, the counter electrodes were heat treated for 30 min at 200 °C in a heating cabinet (B150 muffle oven, Nabertherm, Lilienthal, Germany). This procedure is known to form a graphite catalyst layer in the range of 2–4 µm [13].

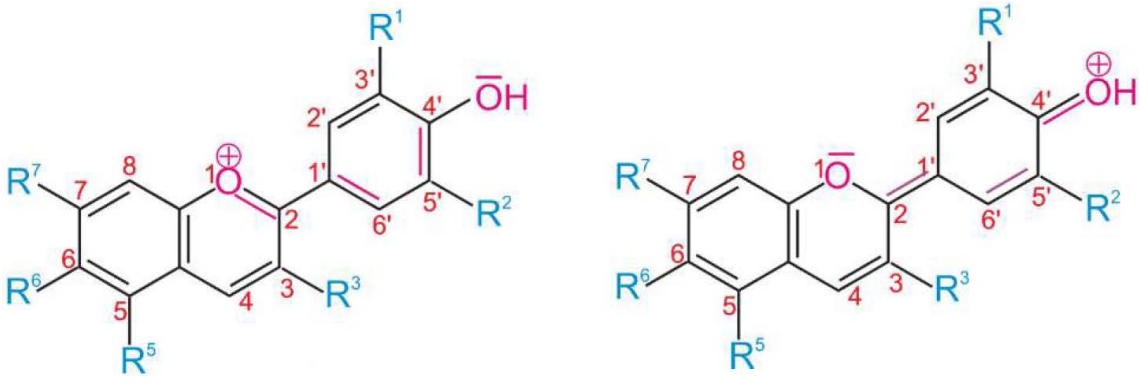


*Figure 1: Mesomeric boundary structures of the anthocyanin backbone. Some of the residues may be bound sugars, for example. However, most of the residues consist of hydroxy groups or hydrogen.*

For assembly, the two prepared glass plates were placed on top of each other with a slight offset for attaching the measuring clamps and fixed tightly by means of adhesive tape. This design provides a DSSC with a reactive area of 6 $cm^2$, which is quite large compared to common cells in literature [14]. A liquid, commercially available electrolyte (ManSolar, Petten, Netherlands) was applied to the cell by capillary force. A total of three DSSCs were built according to this design.

For measurement, the DSSCs were placed under a solar simulator LS0500 with an AM 1.5G spectrum (LOT-Quantum Design GmbH, Darmstadt/Germany) with a power of 100 mW/$cm^2$ and a black, non-reflecting background. The current-voltage characteristics were recorded by a Keithley 2450 sourcemeter. The DSSCs were stored for the rest of the time in the dark under laboratory conditions.

The macroscopic images were taken using a Sony Cybershot DSC-RX100 IV camera. Light microscope images were taken using a Zeiss Axio Observer Microscope in transmissive light mode.

To measure the nanofiber mat by means of SEM, the nanofiber mat was stuck on a Stub via a graphite adhesive pab and thinly sputtered with palladium. All measurements were performed at a high voltage of 10 kV, and secondary electrons were detected.

TGA measurement were made using a Hi-Res TGA 2950 Thermo-gravimetric Analyzer from TA Instruments (New Castle, DE, USA) under a constant air flow and a temperature increase of 10 K/min from 40 °C to 800 °C.

## 3 Results and discussion

Figure 2 shows a) an untreated $TiO_2$ nanofiber mat after the spinning process; b) a pure X-PAN mat after dip-coating in an anthocyanin dye solution and subsequent drying in the dark; and c) a $TiO_2$ nanofiber mat dyed analogously. The white colour of the untreated nonwoven is due to the polymer and $TiO_2$, which is also a known bleaching agent. In clear contrast, the dyed nonwovens show a distinct coloration. Nanofiber mat c) with $TiO_2$ shows a clearly darker coloration than sample b). This indicates the expected bathochromic shift, also known as red shift, in the spectrum due to the bond between anthocyanin and $TiO_2$ [4]. The smaller, even darker particles on the dyed nonwovens are solid residues from the dissolution process of the anthocyanin from the tea, which could not be completely filtered out.

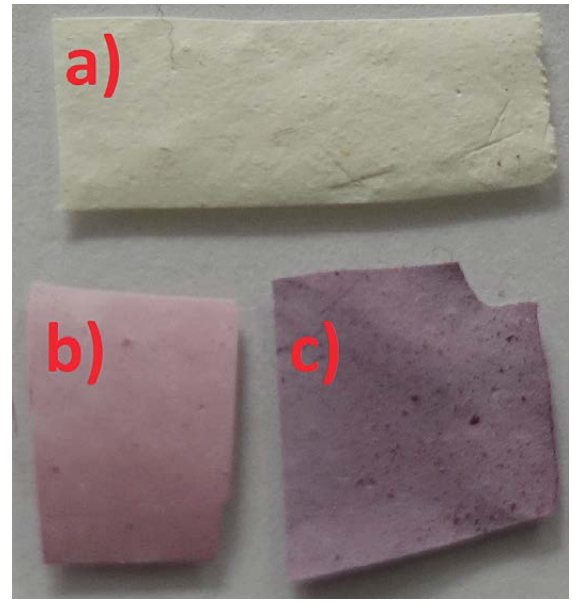


*Figure 2: Photograph of differently treated electrospun nanofiber mats: a) PAN-$TiO_2$ without further treatment; b) pure PAN after dip-coating in a anthocyanin dye solution and drying; and c) PAN-$TiO_2$ after dyeing*

Figure 3 shows light microscope images of the nanofiber mat in a) and b) untreated state and c) and d) after dip-coating, and drying in transmitted light mode with a magnification factor of around 10 between images a) and b) and c) and d). The thickness of the nanofiber mat appears to vary in different positions, which is evident from the lighter and darker areas in images a) and c), which acts as a background for the much darker particles. In Figures 2 b) and d), nanofibers are already visible, and have a diameter of up to 1.6 µm, although the diameter of most fibres is less than 1 µm. In addition, large accumulations of $TiO_2$ can be seen in the images, which in isolated cases have diameters of up to 50 µm.

In the optical comparison of the uncoloured nanofiber mats (Figure 3 a) and b)) with the coloured mat images (c) and d)), it is clear that the colouring and thus binding of the anthocyanin dye takes place on the $TiO_2$ particles and nanofibers containing $TiO_2$ nanoparticles.

Figure 4 shows SEM images of the untreated nanofiber mat containing PAN and $TiO_2$, with increasing magnification from a) to d). Here, $TiO_2$ accumulations can also be seen in all four images,

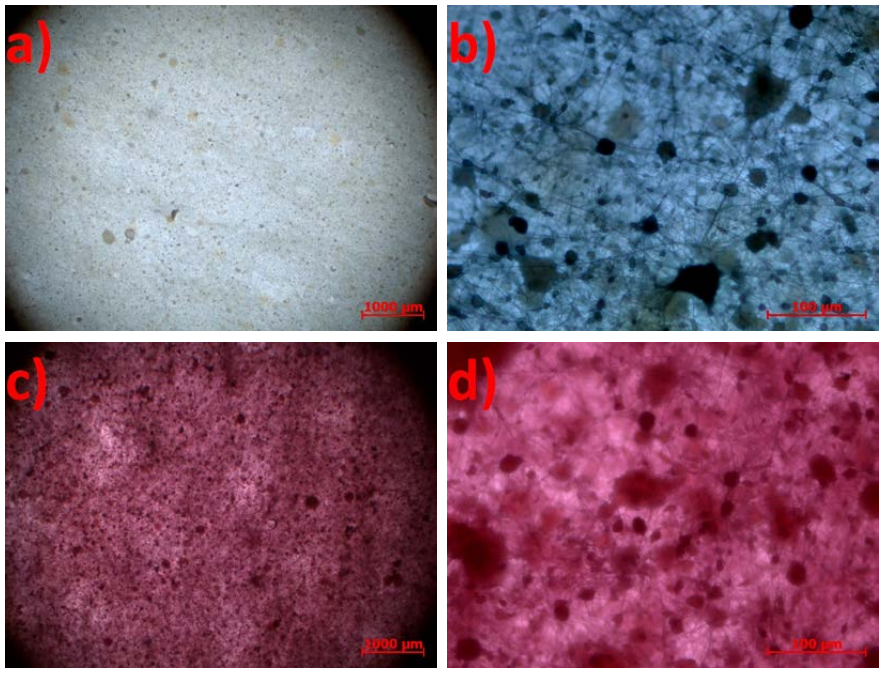


*Figure 3: Light microscope images of the PAN-$TiO_2$ nanofiber mats a) and b) before dyeing; and c) and d) after dyeing with different magnifications*

and appear to be very disordered and vary greatly in size. While the larger $TiO_2$ particles, which are up to 10 µm in size, are in the nanofiber mat and partly act as anchor and starting points for nanofibers, the smaller particles are located around and on the nanofibers, and do not interrupt the nanofiber structure.

The diameter of the nanofibers varies greatly, from 90 nm to about 1.5 µm, as previously suspected in Figure 3. Here, it is possible that even thinner fibres exist that either cannot be resolved or appear thicker due to a $TiO_2$ cladding. Particularly in needle electrospinning, particles seem to negatively influence the spin behaviour and thus lead to a large

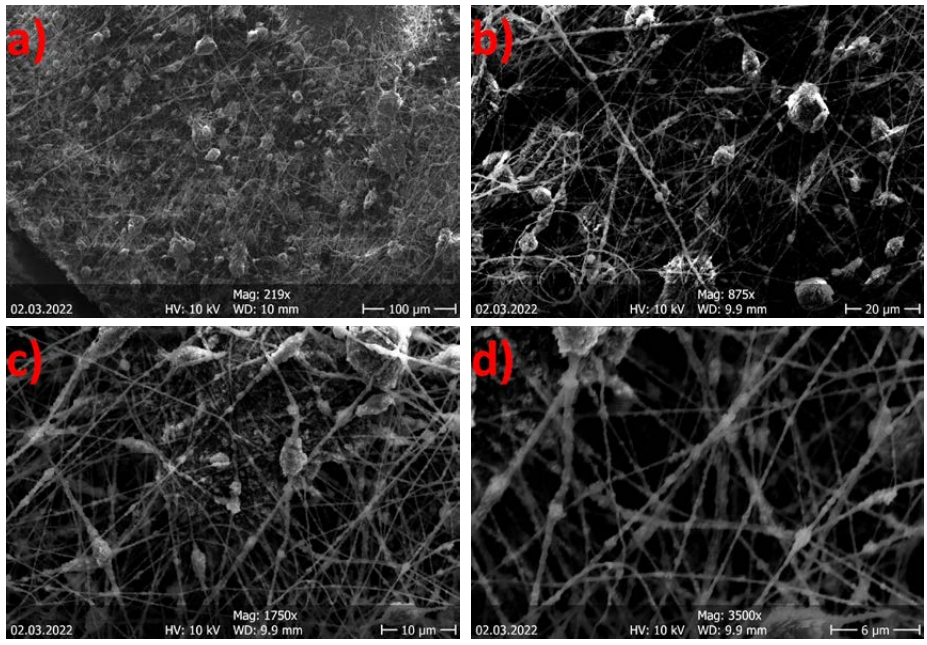


*Figure 4: REM images of the undyed PAN-$TiO_2$ nanofiber mat with increasing magnification from a) to d).*

variation in nanofiber diameter, while for a fixed DMSO:PAN ratio, the fibre thickness varies little, as described by Grothe et al [15, 16].

Due to the spinning process using a movable nozzle holder and rotating collector roll, the nanofibers should have a preferred direction. This cannot be identified with certainty on the basis of SEM images of Figure 4 a) to d), although in image a) the diagonal from bottom left to top right can be assumed to be the most probable.

Figure 5 shows the TGA measurement of the uncoloured PAN-$TiO_2$ nanofiber mat. The first range up to about 300 °C shows only a slight, steady decrease of 3 to 4 % due to the evaporation of water. At 300 °C, the melting point of PAN is reached and volatile gases are released, which lead to an abrupt decrease in weight by 18% [17, 18]. In this range and even up to 600 °C, the further combustion of organic components and evaporation of $NH_3$ and HCN takes place, resulting in a steady decrease of 32% [19]. Subsequently, 46% of the initial mass remains, which resembles the $TiO_2$ content, as this only melts and evaporates at significantly higher temperatures. Thus, the mass content of about 46% $TiO_2$ in the nanofiber mat corresponds to the ratio of the mass proportions of PAN and $TiO_2$ (1:1) in the spinning suspension.

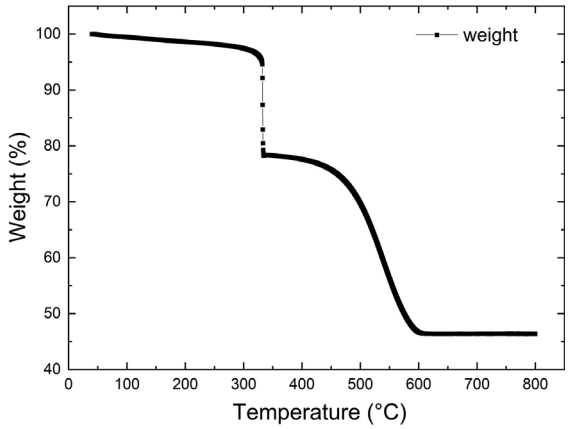


*Figure 5: TGA measurement of the undyed PANTi$O_2$ nanofiber mat*

Figure 6 shows the measured efficiencies of the three constructed DSSCs, where instead of the individual efficiencies per measurement day, the mean value of these is given with a standard deviation. This plot was chosen because there were isolated, presumably erroneous measurements of the respective cells as is known for the conductive glass plates used [9]. However, these measurement errors are taken into account and are reflected in the occasionally very large standard deviations. If the whole curve is considered in a physical context, a rather straight-line progression can be assumed, supported by several similar values with very small standard deviations.

Considering the pure mean values, efficiency increases during the first week from around 0.0003% to an average of 0.0012%, but fluctuates after three weeks with efficiencies ranging from 0.0002% to 0.0007%. Including the standard deviation, an efficiency of 0.0003% seems to be acceptable as a plausible value for the later course and is thus equal to the first measurement.

The fact that electrospinning can also be used to produce DSSCs with higher efficiencies has been shown several times in literature. Osfouri et al. describe a DSSC with electrospun $TiO_2$ nanofibers doped by bio-Ca nanoparticles with up to 1.48% efficiency [20]. DSSC efficiencies of a similar magnitude have been reported by Al-Alwani et al. [21] (0.23% effectivity) and Prabavathy et al. [22] with 0.99% to 1.17%. The impact of the pH value during extraction was shown by Ekpunobi et al. [23], with a pH value of three leading to an efficiency of 0.98%. Higher efficiencies can also be achieved with ruthenium dyes. Nien et al. [24] achieved efficiencies of between 3.11% and 7.92%, varying the light intensity on the one hand and the addition of $ZnFe_2O_4$ on the other.

In the work of Kohn et al. [3], DSSCs spun with dye and subsequently made conductive with PEDOT:PSS achieved efficiencies on the order of $10^{-3}$ %. A similar procedure to that described here by Mamun et al. [12], but in which the nonwovens were carbonized and then dyed, resulted in an efficiency of 0.0001%. In these two tests, however, the DSSC was measured at most up to the seventh day and no long-term stability was proven. We were able to confirm comparable efficiencies with the needle electrospinning and simpler production of the DSSCs over a period of 60 days. Furthermore, the efficiency is low compared to DSSCs with completely nontoxic, inexpensive materials that are known to have low efficiencies, whereby the measurement issues already mentioned above will have some influence in this regard [8, 9, 25]. To the best of our knowledge, this report is the first to show DSSCs that are made of a $TiO_2$ nanofiber mat that has not been subsequently sintered, carbonized or otherwise made conductive. In particular, the sintering of the $TiO_2$ layer is necessary for conventional cells.

It can be assumed that the future optimization of the nanofiber mat, especially with regard to contact to other layers of the cell, will lead to significant improvements in efficiency.

It is interesting to compare this with DSSCs that use the same commercial electrolyte and also have the same materials as components. With these normal cells, the efficiency is generally higher due to the fact that they were built as a comparison to other DSSCs, in which various aspects were changed and investigated. As a rule, these cells are significantly higher in terms of efficiency at the beginning of the measurements than other DSSCs, which, for example, test other electrolytes. However, these DSSCs with the commercial electrolyte already drop sharply after a few days and are sometimes no longer active after two months [9, 10, 25]. In contrast, Figure 6 shows a very low but nearly constant efficiency. In the optimum case, this could indicate that the evaporation of the electrolyte is reduced by this type of front electrode. As a negative interpretation, it would also be acceptable that the effect of evaporation would not play a major role at such a low efficiency. In any case, this is an observation that should be investigated through further long-term measurements.

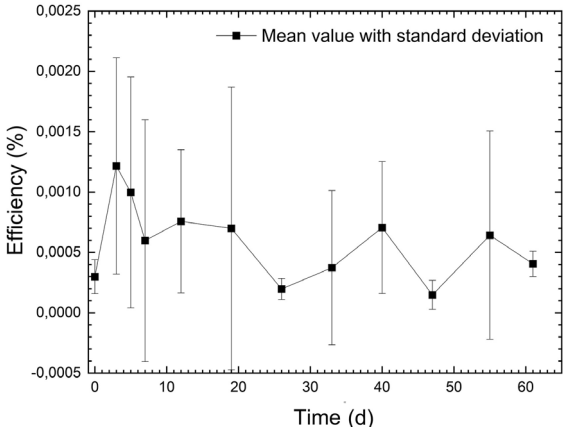


*Figure 6: Mean values and standard deviations over 61 days of the three manufactured DSSCs with a needle electrospun and dyed nanofiber mat as front electrode*

## 4 Conclusion

The electrospun nanofiber mat containing PAN as a polymer and $TiO_2$ nanoparticles was characterized via optical microscopy and REM, which showed that the nanofibers and $TiO_2$ nanoparticles varied greatly in size and distribution. The nanofiber mat was then dyed using a solution of water, ethanol and extracted anthocyanin. A comparison with a $TiO_2$-free, dyed nanofiber mat shows a clear red shift, confirming the bonding of the dye to the semiconductor material. The DSSCs built with the nanofiber mat as the front electrode showed a low but roughly constant efficiency over two months of measurement. Given that the nanofiber mat was not sintered and only low cost, non-toxic ingredients where used, the results are promising, but still require significant optimization.

For future studies, a comparison with a needleless electrospun nanofiber mat, whose spin solution has similar concentrations, would also be conceivable. The alignment of the nanofibers was not detected in anyway by the constellation used here.

### Funding

*This research was partly funded by the German Federal Ministry for Economic Affairs and Climate Action via the AiF, based on a resolution of the German Bundestag, grant number KK5044902SY0.*

### Conflicts of Interest

*The authors declare no conflict of interest. The funders had no role in the design of the study, in the collection, analyses or interpretation of data, in the writing of the manuscript or in the decision to publish the results.*

## References

1. DRESSELHAUS, M.S., THOMAS, I.L. Alternative energy technologies. *Nature*, 2001, **414**, 332–337, doi: 10.1038/35104599.
2. *Renewables 2020*. Paris : OECD, 2020, doi: 10.1787/c74616c1-en.
3. KOHN, S., WEHLAGE, D., JUHÁSZ JUNGER, I., EHRMANN, A. Electrospinning a dye-sensitized solar cell. *Catalysts*, 2019, **9**(12), 1–9, doi: 10.3390/catal9120975.
4. O'REGAN, B., GRÄTZEL, M. A low-cost, high-efficiency solar cell based on dye-sensitized colloidal $TiO_2$ films. *Nature*, 1991, **353**, 737–740, doi: 10.1038/353737a0.
5. MUÑOZ-GARCÍA, A.B., BENESPERI, I., BOSCHLOO, G., CONCEPCION, J.J., DELCAMP, J.H., GIBSON, E.A., MEYER, G.J., PAVONE, M., PETTERSSON, H., HAGFELDT, A., et al. Dye-

sensitized solar cells strike back. *Chemical Society Reviews*, 2021, **50**(22), 12450–12550, doi: 10.1039/D0CS01336F.

6. SCHODEN, F., DOTTER, M., KNEFELKAMP, D., BLACHOWICZ, T., SCHWENZFEIER HELLKAMP, E. Review of state of the art recycling methods in the context of dye sensitized solar cells. *Energies*, 2021, **14**(13), 1–12, doi: 10.3390/en14133741.
7. EHRMANN, A., BLACHOWICZ, T. Recent coating materials for textile-based solar cells. *AIMS Materials Science*, 2019, **6**(2), 234–251, doi: 10.3934/matersci.2019.2.234.
8. GOSSEN, K., DOTTER, M., BROCKHAGEN, B., STORCK, J.L., EHRMANN, A. Long-term investigation of unsealed DSSCs with glycerol-based electrolytes of different compositions. *AIMS Materials Science*, 2022, **9**(2), 283–296, doi: 10.3934/matersci.2022017.
9. STORCK, J.L., DOTTER, M., BROCKHAGEN, B., GROTHE, T. Evaluation of novel glycerol/PEO gel polymer electrolytes for non-toxic dye-sensitized solar cells with natural dyes regarding long-term stability and reproducibility. *Crystals*, 2020, **10**(12), 1–15, doi: 10.3390/cryst10121158.
10. DOTTER, M., STORCK, J.L., SURJAWIDJAJA, M., ADABRA, S., GROTHE, T. Investigation of the long-term stability of different polymers and their blends with PEO to produce gel polymer electrolytes for non-toxic dye-sensitized solar cells. *Applied Sciences*, 2021, **11**(13), 1–14, doi: 10.3390/app11135834.
11. GROTHE, T., STORCK, J.L., DOTTER, M., EHRMANN, A. Impact of solid content in the electrospinning solution on the physical and chemical properties of polyacrylonitrile (PAN) nanofibrous mats. *Tekstilec*, 2020, **63**(3), 225–232, doi: 10.14502/Tekstilec2020.63.225-232.
12. MAMUN, A., TRABELSI, M., KLÖCKER, M., SABANTINA, L., GROßERHODE, C., BLACHOWICZ, T., GRÖTSCH, G., CORNELIßEN, C., STREITENBERGER, A., EHRMANN, A. Electrospun nanofiber mats with embedded non-sintered $TiO_2$ for dye-sensitized solar cells (DSSCs). *Fibers*, 2019, **7**(7), 1–10, doi: 10.3390/fib7070060.
13. JUHÁSZ JUNGER, I., GROSSERHODE, C., STORCK, J.L., KOHN, S., GRETHE, T., GRASSMANN, C., SCHWARZ-PFEIFFER, A., GRIMMELSMANN, N., MEISSNER, H., BLACHOWICZ, T., et al. Influence of graphite-coating methods on the DSSC performance. *Optik*, 2018, **174**, 40–45, doi: 10.1016/j.ijleo.2018.08.041.
14. UDOMRUNGKHAJORNCHAI, S., JUNGER, I.J., EHRMANN, A. Optimization of the $TiO_2$ layer in DSSCs by a nonionic surfactant. *Optik*, 2020, **203**, 163945, doi: 10.1016/j.ijleo.2019.163945.
15. GROTHE, T., WEHLAGE, D., BÖHM, T., REMCHE, A., EHRMANN, A. Needleless Electrospinning of PAN Nanofibre Mats. *Tekstilec*, 2017, **60**(4), 290–295, doi: 10.14502/Tekstilec2017.60.290-295.
16. STORCK, J.L., GROTHE, T., MAMUN, A., SABANTINA, L., KLÖCKER, M., BLACHOWICZ, T., EHRMANN, A. Orientation of electrospun magnetic nanofibers near conductive areas. *Materials*, 2019, **13**(1), 1–14, doi: 10.3390/ma13010047.
17. LEE, S., KIM, J., KU, B.-C., KIM, J., JOH, H.-I. Structural evolution of polyacrylonitrile fibers in stabilization and carbonization. *Advances in Chemical Engineering and Science*, 2012, **2**(2), 275–282, doi: 10.4236/aces.2012.22032.
18. KIM, H.M., CHAE, W.-P., CHANG, K.-W., CHUN, S., KIM, S., JEONG, Y., KANG, I.-K. Composite nanofiber mats consisting of hydroxyapatite and titania for biomedical applications. *Journal of Biomedical Materials Research Part B: Applied Biomaterials*, 2010, **94B**(2), 380–387, doi: 10.1002/jbm.b.31664.
19. ALARIFI, I.M., ALHARBI, A., KHAN, W.S., SWINDLE, A., ASMATULU, R. Thermal, electrical and surface hydrophobic properties of electrospun polyacrylonitrile nanofibers for structural health monitoring. *Materials*, 2015, **8**(10), 7017–7031, doi: 10.3390/ma8105356.
20. GOLSHAN, M., OSFOURI, S., AZIN, R., JALALI, T., MOHEIMANI, N.R. Efficiency and stability improvement of natural dye-sensitized solar cells using the electrospun composite of $TiO_2$ nanofibres doped by the bio-Ca nanoparticles. *International Journal of Energy Research*, 2022, **46**(11), 15407–15418, doi: 10.1002/er.8242.
21. AL-ALWANI, M.A.M., AL-MASHAAN, A.B.S.A., ABDULLAH, M.F. Performance of the dye-sensitized solar cells fabricated using natural dyes from *Ixora coccinea* flowers and *Cymbopogon schoenanthus* leaves as sensitizers. *International Journal of Energy Research*, 2019, **43**(13), 7229–7239, doi: 10.1002/er.4747.
22. PRABAVATHY, N., SHALINI, S., BALASUNDARAPRABHU, R., VELAUTHAPILLAI, D.,

PRASANNA, S., BALAJI, G., MUTHUKUMARASAMY, N. Algal buffer layers for enhancing the efficiency of anthocyanins extracted from rose petals for natural dye-sensitized solar cell (DSSC). *International Journal of Energy Research*, 2018, **42**(2), 790–801, doi: 10.1002/er.3866.

23. EKPUNOBI, U.E., OGBUEFI, S.I., EKPUNOBI, A.J. Dye pH effect on photoelectric parameters of natural photosensitizer pigment extracted from *Alstonia boonei* for dye-sensitized solar cells. *International Journal of Energy Research*, 2022, **46**(2), 1922–1933, doi: 10.1002/er.7307.
24. NIEN, Y.-H., WU, Y.-T., CHOU, J.-C., YANG, P.-H., HO, C.-S., LAI, C.-H., KUO, P.-Y., SYU, R.-H., ZHUANG, S.-W., CHEN, P.-F. Photovoltaic performance of dye-sensitized solar cells under low illumination by modification of a photoanode with $ZnFe_2O_4/TiO_2$ nanofibers. *IEEE Transactions on Nanotechnology*, 2022, **21**, 606–612, doi: 10.1109/TNANO.2022.3213278.
25. STORCK, J.L., DOTTER, M., ADABRA, S., SURJAWIDJAJA, M., BROCKHAGEN, B., GROTHE, T. Long-term stability improvement of non-toxic dye-sensitized solar cells ia poly(ethylene oxide) gel electrolytes for future textile-based solar cells. *Polymers*, 2020, **12**(12), 1–15, doi: 10.3390/polym12123035.